Inorganic Chemistry
Article

Inorg. Chem. **2009**, *48*, 8271–8275 **8271**
DOI: 10.1021/ic9009114

Nature of Insulating-Phase Transition and Degradation of Structure and Electrochemical Reactivity in an Olivine-Structured Material, $LiFePO_4$

Min-Sang Song,[†,∥] Yong-Mook Kang,[*,‡] Yong-Il Kim,[§] Kyu-Sung Park,[∥] and Hyuk-Sang Kwon[*,†]

[†]*Department of Materials Science and Engineering, Korea Advanced Institute of Science and Technology, 373-1 Guseong-Dong, Yuseong-gu, Daejeon, 305-701, Republic of Korea,* [‡]*Division of Advanced Materials Engineering, Kongju National University, 275 Budae-dong, Cheonan, Chungnam, Republic of Korea,* [§]*Korea Research Institute of Standards and Science, P.O. Box 102, Yuseong, Daejeon, Republic of Korea, and* [∥]*Battery Group, Emerging Center, Samsung Advanced Institute of Technology, San 14-1 Nongseo-dong, Giheung-gu, Yongin-si, Gyeonggi-do, 446-712, Republic of Korea*

Received May 11, 2009

Synthesis time using microwave irradiation was varied to elucidate the electrochemical degradation mechanism of $LiFePO_4$ related to the evolution of Fe_2P. When the amount of Fe_2P was above a critical level, $LiFePO_4$ tended to change into an insulating phase, $Li_4P_2O_7$. The correlation between structural analysis and electrochemical analysis attributed the initial degradation of $LiFePO_4$ to the low electronic conductivity of $Li_4P_2O_7$, whereas the deficiency of P and O evolved by $Li_4P_2O_7$ resulted in the cyclic degradation of $LiFePO_4$. This kind of correlation between structure and electrochemical performance in intercalation materials will significantly contribute to an explanation of their degradation mechanism for their application.

Introduction

$LiFePO_4$, with an olivine structure, has been spotlighted as a promising candidate cathode material due to its excellent thermal stability, the low cost of its precursors, the high reversibility of Li insertion/extraction, and a lack of toxicity.[1−3] Although $LiFePO_4$ has an inherent poor kinetic property ($\sigma_e = 10^{-8}$ S cm^{-1} (low electronic conductivity), $D_{Li^+} = 10^{-14}$ cm^2 s^{-1} at room temperature (rt; low Li^+ diffusivity)),[4,5] a marvelous improvement in its kinetic property was achieved during the past decade with the help of carbon coating ($LiFePO_4$/C composite),[6−11] particle size reduction,[5,12,13] and supervalent cation doping.[14] Actually, the electrochemical enhancement coming from these strategies made $LiFePO_4$ a feasible cathode material for commercialization.

In the early stage of $LiFePO_4$ research, Fe_2P, formed in a strong reductive atmosphere, was considered as a byproduct which should be prevented from forming during the synthesis of single-phase $LiFePO_4$.[12] However, Subramanya Herle et al. demonstrated that metal phosphocarbides or Fe_2P (metallic compound, σ: 10^{-1} S cm^{-1} at rt) can contribute to improving the room-temperature conductivity of $LiFePO_4$/C drastically to $\sim 10^{-2}$ S cm^{-1} thanks to its high electronic conductivity.[15] Recently, Xu et al. verified the positive effect of Fe_2P on the electrochemical performance of $LiFePO_4$ by showing that $LiFePO_4$ including Fe_2P has the best rate capability in spite of having the largest particle size.[16] However, our previous study demonstrated that the formation of Fe_2P can result in amphoteric effects on the electrochemical performance of $LiFePO_4$ depending on its quantity.[17]

*Corresponding author. Tel.: +82-16-257-9051 (Y.M.K.). Fax: +82-41-568-5776 (Y.M.K.). E-mail: dake1234@kongju.ac.kr (Y.M.K.), hskwon@kaist.ac.kr (H.S.K.).

(1) Giorgetti, M.; Berretoni, M.; Scaccia, S.; Passerini, S. *Inorg. Chem.* **2006**, *45*, 2750.
(2) Tarascon, J. M.; Armand, M. *Nature* **2001**, *414*, 359.
(3) Yamada, A.; Chung, S. C.; Hinokuma, K. *J. Electrochem. Soc.* **2001**, *148*, 224.
(4) Chung, S. Y.; Chiang, Y. M. *Electrochem. Solid-State Lett.* **2003**, *6*, 278.
(5) Prosini, P. P.; Carewska, M.; Scaccia, S.; Wisniewski, P.; Pasquali, M. *Electrochim. Acta* **2003**, *48*, 4205.
(6) Gabrisch, H.; Wilcox, J. D.; Doeff, M. M. *Electrochem. Solid-State Lett.* **2006**, *9*, 360.
(7) Ravet, N.; Chouinard, Y.; Magnan, J. F.; Besner, S.; Gauthier, M.; Armand, M. *J. Power Sources* **2001**, *97−98*, 503.
(8) Chung, H. T.; Jang, S. K.; Ryu, H. W.; Shim, K. B. *Solid State Commun.* **2004**, *131*, 549.
(9) Huang, H.; Yin, S. C.; Nazar, L. F. *Electrochem. Solid-State Lett.* **2001**, *4*, 170.
(10) Chen, Z.; Dahn, J. R. *J. Electrochem. Soc.* **2002**, *149*, 1184.
(11) Franger, S.; Bourbon, C.; Le Cras, F. *J. Electrochem. Soc.* **2004**, *151*, 1024.
(12) Arnold, G.; Garche, J.; Hemmer, R.; Ströbele, S.; Vogler, C.; Wohlfahrt-Mehrens, M. *J. Power Sources* **2003**, *119−121*, 247.
(13) Prosini, P. P.; Carewska, M.; Scaccia, S.; Wisniewski, P.; Passerini, S.; Pasquali, M. *J. Electrochem. Soc.* **2002**, *149*, 886.
(14) Chung, S. Y.; Bloking, J. T.; Chiang, Y. M. *Nat. Mater.* **2002**, *1*, 123.
(15) Subramanya Herle, P.; Ellis, B.; Coombs, N.; Nazar, L. F. *Nat. Mater.* **2004**, *3*, 147.
(16) Xu, Y.; Lu, Y.; Yan, L.; Yang, Z.; Yang, R. *J. Power Sources* **2006**, *160*, 570.
(17) Song, M. S.; Kim, D. Y.; Kang, Y. M.; Kim, Y. I.; Kwon, H. S.; Lee, J. Y. *J. Power Sources* **2008**, *108*(1), 546.

Published on Web 08/05/2009

Generally, in previous reports, $LiFePO_4$ including Fe_2P below the critical amount displayed an enhanced electrochemical performance, whereas Fe_2P inclusion above the critical amount seriously deteriorated the electrochemical performance of $LiFePO_4$. The positive effect of Fe_2P below the critical amount has been easily ascribed to Fe_2P-induced enhancement of electronic conductivity in $LiFePO_4$ because Fe_2P is electronically conductive. The reason why $LiFePO_4$ with Fe_2P above the critical amount has to undergo a significant degradation is assumed to be related to the Li^+ pathway being blocked by an excessive formation of Fe_2P in $LiFePO_4$. Considering that the application (HEV, plug-in HEV, and EV) of $LiFePO_4$ requires high rate capability, the detailed change of the $LiFePO_4$ structure with the variation of the Fe_2P amount should be clarified in the first place for its commercialization.

So, in this paper, the effect of Fe_2P formation on the local structure of $LiFePO_4$ was correlated with the electrochemical performance of $LiFePO_4$. For this, the local structure of $LiFePO_4$ was comprehensively analyzed with variation of the Fe_2P amount.

Experimental Section

Synthesis. $LiFePO_4$ (including carbon web) was synthesized by ball-milling and subsequent microwave heating. A stoichiometric amount (1:1, molar ratio) of Li_3PO_4 (Aldrich) and $Fe_3(PO_4)_2 \cdot 8H_2O$ (Kojundo) was ball-milled at a ball-to-powder weight ratio of 8.10:1 with 5 wt % acetylene black for 30 min under an Ar atmosphere using a vibrant-type mill (SPEX-8000 mixer/mill), and then the ball-milled mixture was microwave irradiated (750 W) for several minutes in a microwave oven.

Cell Fabrication. $LiFePO_4$ cathodes were manufactured by casting, on an Al foil current collector, a *N*-methyl-2-pyrrolidene slurry composed of 72 wt % $LiFePO_4$−C, 20 wt % acetylene black, and 8 wt % polyvinylidene fluoride binder. A total of 2016 coin-type cells were assembled in an Ar-filled glovebox by stacking a microporous polypropylene separator (Celgard 2400) containing liquid electrolyte (1 M $LiClO_4$ in 1:1 EC/DMC) between the cathode and the lithium metal foil anode.

Structural and Electrochemical Analyses. Two- and three-phase Rietveld refinements for $LiFePO_4$ (including carbon web) were conducted using the General Structure Analysis System program.[18] The X-ray diffraction (XRD) data for Rietveld refinement were measured from 15° to 120° at a step of 0.02° using Cu Kα radiation with a graphite monochromator in the reflection geometry (Dmax2200 V, Rigaku). Si (NIST 640c) powder was used as an external standard to correct the zero-point shift for the measured diffraction data. The coordination number of atoms around the Fe atom in $LiFePO_4$ was evaluated by extended X-ray absorption fine structure (EXAFS, *R*-XAS) spectroscopy. Fe K-edge X-ray absorption spectra were recorded in the transmission mode at room temperature using the lab-scale EXAFS machine equipped with a 3 kW X-ray generator, Mo target, W filament, and Ge(220) crystal. The X-ray absorption spectra were Fourier-transformed using the IFEFFIT program based on FEFF8 ab inito theory. An ex situ XRD analysis (D/max-III C, Rigaku) of the $LiFePO_4$ (including carbon web) cathode after cycling was conducted from 15° to 45° at a scan rate of 1° min^{-1} using Cu Kα radiation. Electrochemical impedance spectroscopy (EIS) analysis was conducted at room temperature using a HF frequency response analyzer (SI1255, solartron instruments) connected to a potentiostat/galvanostat (273A, EG&G Princeton Applied Research). A small AC perturbation of 10 mV was applied with a frequency sweep from 0.1 Hz to 100 kHz during the measurements. The amount of iron dissolved from $LiFePO_4$ to the electrolyte in a cell was measured with an inductively coupled plasma mass spectrometer (ICP-MASS, Elan 6100, Perkin-Elmer).

(18) Larson, A. C.; Von Dreele, R. B. *Los Alamos National Laboratory Report LAUR*; Los Alamos National Laboratory: Los Alamaos, NM, **1994**; p 86.

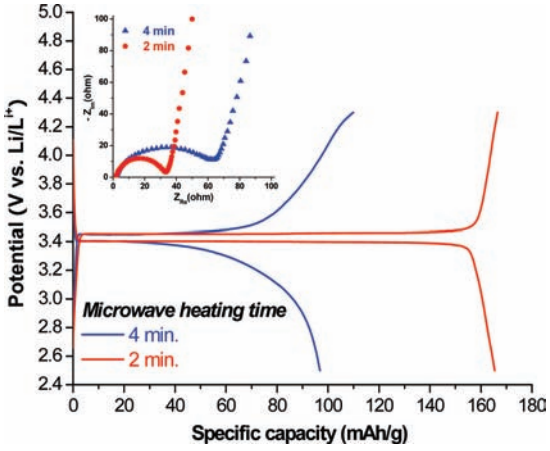

Figure 1. The initial charge/discharge curves of $LiFePO_4$ synthesized by microwave irradiation for 2 min (red-colored line) and 4 min (blue-colored line). Inset figure consists of Nyquist plots for 2-min-irradiated $LiFePO_4$ (red-colored sphere) and 4-min-irradiated $LiFePO_4$ (blue-colored triangle).

Results and Discussion

The initial electrochemical reactivity of $LiFePO_4$ (including carbon web) synthesized from microwave irradiation is displayed in Figure 1. In the discharge curve for $LiFePO_4$ prepared by microwave heating for 2 min, a long, flat voltage plateau appears around 3.41 V, and then the voltage sharply drops to the cutoff value (2.5 V), leading to a high discharge capacity of 165 mAh g^{-1} (97.1% of the theoretical capacity of $LiFePO_4$). On the other hand, $LiFePO_4$ obtained by microwave heating for 4 min shows shorter voltage plateaus, followed by a low discharge capacity (97 mAh g^{-1}). An EIS analysis was carried out to investigate the change of charge-transfer resistance in $LiFePO_4$ with the variation of microwave heating time. As shown in the inset of Figure 1, the longer the microwave heating time for the synthesis of $LiFePO_4$, the larger the charge-transfer resistance between the electrolyte and $LiFePO_4$ surface. Because the increase of microwave heating time was correlated with the evolution of Fe_2P, an extremely conductive phase (Figure S1, Supporting Information), a surge of charge-transfer resistance in the 4 min sample may imply that there is another phase transition explanatory of the electrochemical degradation of $LiFePO_4$.

In order to clarify the reason why the 4 min sample encountered difficulty in the charge transfer leading to its electrochemical degradation, the local structure (lattice parameter, space of Li^+ diffusion path, occupation of Fe atoms in the Li site) of $LiFePO_4$ was probed using X-ray Rietveld refinement. Figure 2a shows the refinement results for $LiFePO_4$ irradiated for 2 min.[17] Herein, two phases are observed, 0.56 wt % Fe_2P and 99.44 wt % $LiFePO_4$, and the lattice parameters of $LiFePO_4$ from the refinement (Table S1, Supporting Information) are almost equal to those reported

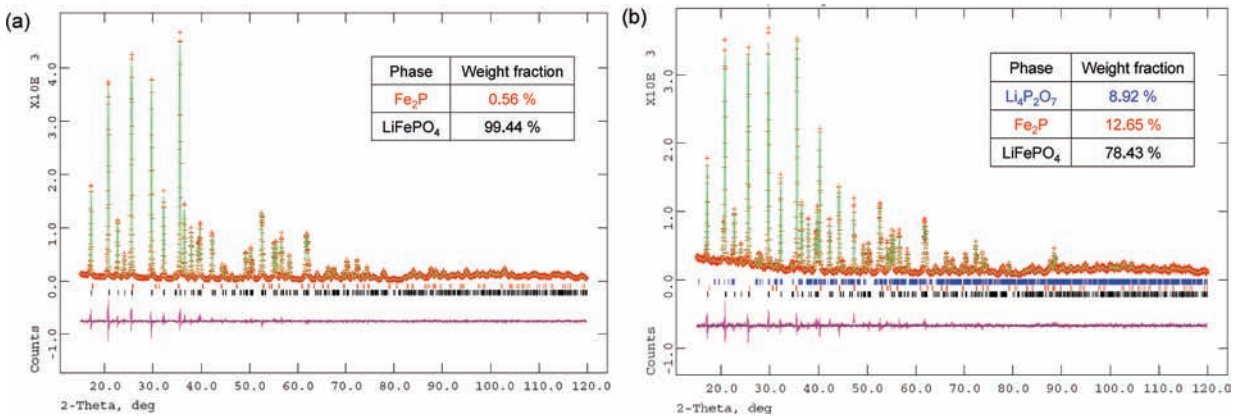

Figure 2. X-ray Rietveld refinement results for $LiFePO_4$ synthesized by microwave irradiation for (a) 2 min and (b) 4 min. Plus (+) marks represent the observed intensities, and the solid line illustrates calculated ones. A difference (obsd − cald) plot is shown beneath. Tick marks above the difference data indicate the reflection position. In 2-min-irradiated $LiFePO_4$, the upper and lower tick marks above the difference data indicate the reflection position for Fe_2P and $LiFePO_4$ phases, respectively, and in 4-min-irradiated $LiFePO_4$, the upper, middle, and lower tick marks correspond to $Li_4P_2O_7$, Fe_2P, and $LiFePO_4$, respectively.

in the literature,[19−22] implying that the structure of $LiFePO_4$ irradiated for 2 min is almost perfect. X-ray Rietveld refinement for $LiFePO_4$ irradiated for 4 min discloses a phase transition responsible for the electrochemical degradation observed in Figure 1. The refinement results for $LiFePO_4$ irradiated for 4 min are given in Figure 2b. Three phases were identified: 8.92 wt % $Li_4P_2O_7$, 12.65 wt % Fe_2P, and 78.43 wt % $LiFePO_4$. The drastic increment in the charge-transfer resistance of the 4 min sample can be explained by the formation of $Li_4P_2O_7$ because it has very low electronic conductivity ($\sim 10^{-20}$ S/cm at rt) and lithium-ion conductivity ($\sim 10^{-21}$ S/cm at rt) compared to those of $LiFePO_4$ itself.[23] Actually, it has been reported that the evolution of $Li_4P_2O_7$ deteriorates the lithium-ion conductivity of $Li_{1+X}Ti_{2-X}Al_X(PO_4)_3$ with a NASICON framework.[24] An abrupt formation of an insulating phase, $Li_4P_2O_7$, in $LiFePO_4$ irradiated for 4 min seems to be attributed to the excessive formation of Fe_2P. $LiFePO_4$ exposed to highly reductive atmosphere has to undergo the reduction of Fe below +2, inducing the formation of Fe_2P. Because Fe_2P is an electronically conductive phase, the formation of Fe_2P below a critical amount tends to help the electrochemical performance of $LiFePO_4$ become enhanced. However, an Fe_2P amount above the critical level is accompanied by a deficiency of Fe and P atoms constituting the framework of $LiFePO_4$. Naturally, $LiFePO_4$ should be changed into a mixture of several phases according to the following reaction:

$$4LiFePO_4 \rightarrow Li_4P_2O_7 + 2Fe_2P + \frac{9}{2}O_2$$

Considering that the refinement simulation assuming three phases, $Li_4P_2O_7$, Fe_2P, and $LiFePO_4$, was appropriate for not the 2 min sample but the 4 min sample, we can know that the phase transition to $Li_4P_2O_7$ is not mandatory when the amount of Fe_2P is below 1 wt % of $LiFePO_4$. The comparison between 4-min-irradiated $LiFePO_4$ and 2-min-irradiated $LiFePO_4$ under the refined lattice parameters made us believe that, irrespective of the formation of $Li_4P_2O_7$, the formation of Fe_2P hardly changes the one-dimensional structure of $LiFePO_4$ (Table S2, Supporting Information). The difference between the lattice parameters of two samples is within the error range. Furthermore, the unit cell volume of $LiFePO_4$ is almost in accordance with that (291.1 Å) of $LiFePO_4$ with the perfect olivine structure regardless of the Fe_2P amount.[25] Even if the excessive Fe_2P accompanied by the formation of $Li_4P_2O_7$ deteriorates the charge-transfer resistance of our $LiFePO_4$, Fe atoms seemed to be perfectly ordered in the structure of $LiFePO_4$, and thus, Li^+ motion through the one-dimensional (1D) path in $LiFePO_4$ looked like it was not disturbed, irrespective of the amount of Fe_2P formation. In order to examine the effect of Fe_2P formation on the 1D Li^+ diffusion path composed of the linear chains of edge-shared LiO_6 octahedra, a change in the Li−O interatomic distance was also estimated. The distance between Li and O atoms in $LiFePO_4$ was also within the error range, proving that the excessive Fe_2P formation does not have a mal effect on Li^+ diffusion path in $LiFePO_4$.

On the basis of the structural parameters obtained from X-ray Rietveld refinement, it seemed that the local structure of $LiFePO_4$ is not influenced by Fe_2P formation. However, considering that the peak intensity in XRD patterns of $LiFePO_4$ is dependent on the amount of Fe_2P, as shown in Figure 2, the local structure of $LiFePO_4$ needed to be probed in detail. Therefore, an Fe-edge EXAFS analysis was conducted to determine the coordination of atoms around the Fe atom. Figure 3 displays the Fe-edge EXAFS spectra, where the peak intensity is proportional to the coordination number of atoms around the Fe atom. From the previous report, it could be known that the first sphere, second sphere, and third sphere correspond to the Fe−O bond, Fe−P bond, and Fe−Fe bond, respectively. The EXAFS spectra for 2-min-irradiated $LiFePO_4$ are very similar to those of $LiFePO_4$ having the perfect olivine structure.[26] On the other hand, several

(19) Andersson, A. S.; Kalska, B.; Häggström, L.; Thomas, J. O. *Solid State Ionics* **2000**, *130*, 41.
(20) Cho, T. H.; Chung, H. T. *J. Power Sources* **2004**, *133*, 272.
(21) Prince, A. A. M.; Mylswamy, S.; Chan, T. S.; Liu, R. S.; Hannoyer, B.; Jean, M.; Shen, C. H.; Huang, S. M.; Lee, J. F.; Wang, G. X. *Solid State Commun.* **2004**, *132*, 455.
(22) Scarlet, N. V. Y.; Madsen, I. C.; Cranswick, L. M. D.; Lwin, T.; Groleau, E.; Stephenson, G.; Aylmore, M.; Agron-Olshina, N. *J. Appl. Crystrallogr.* **2002**, *35*, 383.
(23) Burmakin, E. I.; Shekhtman, G. S.; Aparina, E. R.; Korovenkova, E. S. *Sov. Electrochem.* **1992**, *28*, 1014.
(24) Arbi, K.; Mandal, S.; Rojo, J. M.; Sanz, J. *Chem. Mater.* **2002**, *14*, 1091.
(25) Chen, J.; Whittingham, M. S. *Electrochem. Commun.* **2006**, *8*, 855.
(26) Deb, A.; Bergmann, U.; Cramer, S. P.; Cairns, E. J. *Electrochim. Acta* **2005**, *50*, 5200.

serious changes are shown in the atomic coordination numbers of 4-min-irradiated $LiFePO_4$. This phenomenon is because the deficiencies of O, P, and Fe atoms are significant in 4-min-irradiated $LiFePO_4$, which has to undergo a phase transition to a mixture of Fe_2P and an insulating phase, $Li_4P_2O_7$. Because PO_4 tetrahedra are fundamental building blocks for the olivine structure of $LiFePO_4$, a crucial structural instability can be induced by the deficiency of P and O atoms. With the absence of PO_4 tetrahedra, the structure of $LiFePO_4$ must collapse during the charge/discharge process. Figure 4 shows XRD patterns of $LiFePO_4$ before cycling and after 50 cycles. Even after 50 cycles, the initial structure of 2-min-irradiated $LiFePO_4$ was relatively well-maintained, whereas that of the 4-min-irradiated sample underwent a serious degradation. In accordance with EXAFS results, the structural instability of $LiFePO_4$ during cycling could be attributed to the phase transition to the mixture of Fe_2P and an insulating phase, $Li_4P_2O_7$. In Figure 5, it is shown how this structural instability is correlated with the electrochemical degradation of $LiFePO_4$.

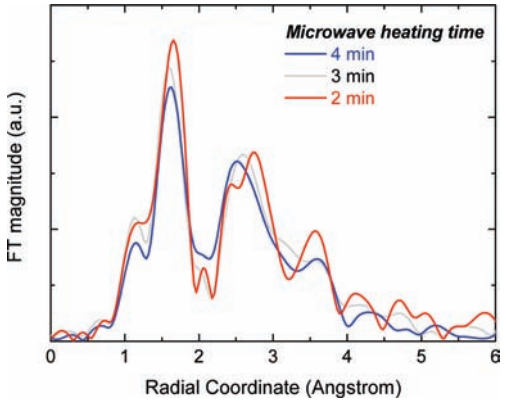

Figure 3. The radial distribution function obtained after Fourier transformation of $k^3\chi(k)$ in the k^3-weighted Fe-edge EXAFS spectrum. First sphere (1.7−2.2 Å), second sphere (2.7−3.2 Å), and third sphere (3.7−4.2 Å) correspond to the Fe−O bond, Fe−P bond, and Fe−Fe bond, respectively.

Figure 5a illustrates the electrochemical superiority of 2-min-irradiated $LiFePO_4$ compared to the 4 min sample. The 2 min sample featured a fabulous cyclic performance in spite of the variation of the charge/discharge rate, while the

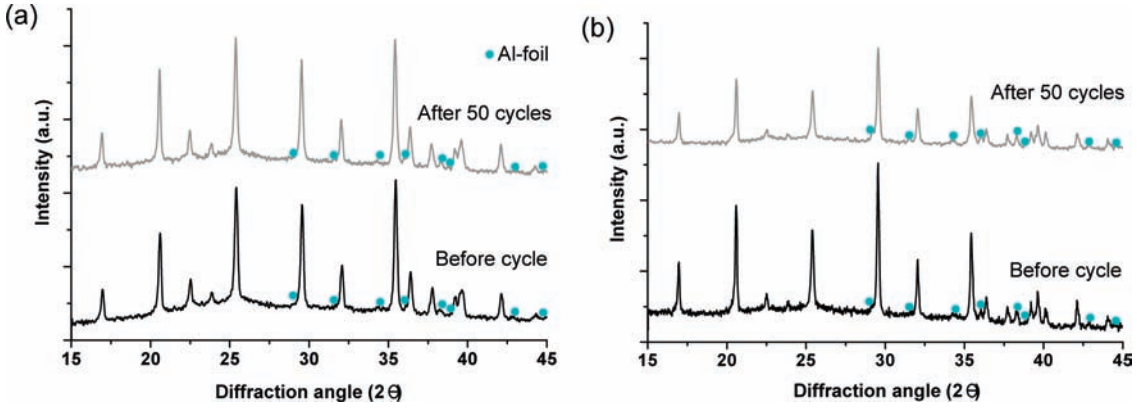

Figure 4. XRD patterns of $LiFePO_4$ before and after cycling: (a) 2 min microwave-irradiated sample, (b) 4 min microwave-irradiated sample.

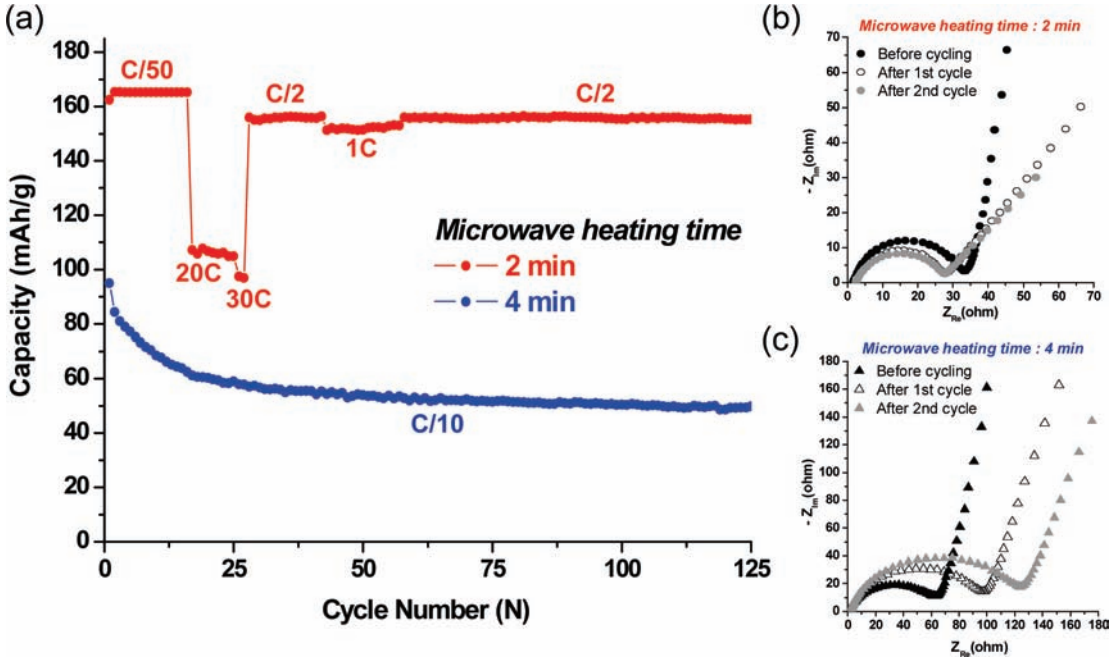

Figure 5. (a) The cyclic properties of $LiFePO_4$ synthesized by microwave irradiation for 2 min (red-colored line) and 4 min (blue-colored line). Nyquist plots for (b) 2-min-irradiated $LiFePO_4$ and (c) 4-min-irradiated $LiFePO_4$ before or after cycling.

4 min sample exhibited poor cyclic performance even at a very sluggish charge/discharge rate (C/10). This tendency in the cyclic performance was consistent with those in the charge/discharge capacity (Figure 1) and the rate capability (Figure S2, Supporting Information). As shown in Figure 5b and c, Nyquist plots obtained during the initial three cycles may correlate the electrochemical performance of $LiFePO_4$ with its local structure. The increase in the charge-transfer resistance of $LiFePO_4$ after cycling mainly comes from Fe dissolution into the electrolyte because the Fe ion dissolved from $LiFePO_4$ goes to an anode and then increases the interfacial impedance of the anode significantly by forming an insulating film on the surface of the anode, as reported by Amine et al.[27] From ICP-MASS analysis (Table S3, Supporting Information), the increment of Fe dissolution is perfectly in accordance with the above-mentioned structural instability coming from the increased Fe_2P formation followed by a phase-transition to $Li_4P_2O_7$. Herein, Fe_2P itself is not the fundamental reason for the increase in the charge-transfer resistance of $LiFePO_4$ during cycling, even if the amount of Fe ions present in the electrolyte is proportional to the amount of Fe_2P. Considering that the local structure change of $LiFePO_4$ depends on the evolution of Fe_2P, it seems to be more reasonable that the electrochemical degradation indicated by the increase of charge-transfer resistance is attributed to the deficiency of P and O evolved by the phase transition into a mixture of Fe_2P and $Li_4P_2O_7$.

(27) Amine, K.; Liu, J.; Belharouak, I. *Electrochem. Commun.* **2005**, *7*, 669.

Conclusion

In conclusion, the evolution of Fe_2P in $LiFePO_4$ above a critical concentration changed $LiFePO_4$ into an insulating phase, $Li_4P_2O_7$. The insulating nature of $Li_4P_2O_7$ leads to the initial degradation of $LiFePO_4$ in spite of the existence of a conducting phase, Fe_2P. The deficiency of P and O in the $LiFePO_4$ framework evolved by the phase transition to the mixture of Fe_2P and $Li_4P_2O_7$ resulted in the structural instability of $LiFePO_4$, which deteriorated its cyclic performance. As a result, the phase transition into $Li_4P_2O_7$ induced by excessive Fe_2P formation brought out a dramatic degradation in the electrochemical properties of $LiFePO_4$, and this degradation mechanism of $LiFePO_4$ suggests the criteria for the synthesis of high-performance $LiFePO_4$ in a reductive atmosphere.

Acknowledgment. The authors acknowledge the Korea Science and Engineering Foundation (KOSEF) grant funded by the Korean government (MEST) (R01-2008-000-11061-0). This research was also supported by the Basic Science Research Program through the National Research Foundation of Korea (NRF) funded by the Ministry of Education, Science and Technology (2009-0072972) and a grant (2009K000186) from the Center for Nanoscale Mechatronics and Manufacturing, one of the 21st Century Frontier Research Programs, which are supported by the Ministry of Education, Science and Technology, Korea.

Supporting Information Available: Additional figures and tables. This material is available free of charge via the Internet at http://pubs.acs.org.